SUPPORTING INFORMATION

Calcium Sensing by Recoverin: Effect of Protein Conformation on Ion Affinity

Štěpán Timr[†,1], Jan Kadlec[†], Pavel Srb[†], O. H. Samuli Ollila[†,‡], and Pavel Jungwirth[†*]

[†]*Institute of Organic Chemistry and Biochemistry, Czech Academy of Sciences, Flemingovo nám. 2, 16610 Prague 6, Czech Republic*

[‡]*Institute of Biotechnology, University of Helsinki, Helsinki, Finland*

[*]*email: pavel.jungwirth@uochb.cas.cz*

[1] Present address: Laboratoire de Biochimie Théorique, CNRS UPR9080, Institut de Biologie Physico-Chimique, Université Paris Diderot, Sorbonne Paris Cité, 13 rue Pierre et Marie Curie, 75005 Paris, France

Supporting Methods

Direct MD simulations

MD simulations were performed using the GROMACS 5.1.2 package.[1] Newton's equations of motion were integrated by employing the leap-frog algorithm[2] with a time step of 2 fs. The trajectory frames were recorded every 2 ps. A cutoff of 1.2 nm was applied to short-range electrostatic interactions while long-range electrostatics was calculated using the particle mesh Ewald method.[3] Van der Waals interactions were truncated at 1.2 nm. Covalent bonds containing hydrogen atoms were constrained by the LINCS algorithm,[4] and water molecules were held rigid by the SETTLE algorithm.[5] The temperature of the system was maintained at 310 K by the velocity rescaling thermostat with a stochastic term,[6] and the Parrinello–Rahman barostat[7] was used with a time constant of 10 ps to keep the system pressure at 1.01 bar. Before the actual production simulations, the maximum forces were decreased below 1000 kJ mol nm^{-1} using the steepest-descent algorithm, and a sequence of three relaxation runs was performed: (1) a 100 ps simulation with all heavy atoms of the protein restrained and a time step of 1 fs, (2) a 1 ns run with all heavy atoms of the protein restrained and with a 2 fs time step, and (3) a 25 ns run with restraints placed on the Cα atoms of the protein backbone and with a 2 fs time step. In all three relaxation steps, the force constant of the harmonic restraints was 1000 kJ mol nm^{-2}, and the Berendsen barostat[8] with a coupling constant of 1 ps was used. The first 100 ns of the production trajectories were not used for structure analysis.

REST2 simulations

Two replica-exchange with solute tempering (REST2) simulations[9] of Ca^{2+}-free recoverin were conducted: one for the semi-open state and the other for the closed state. In both simulations, the solute, i.e., the effectively heated part of the system, was formed by the EF3 loop (residues 110–121). The REST2 simulations were performed in the GROMACS 5.1.4 software[1] patched with the PLUMED 2.3.0 package.[10] For the Ca^{2+}-free semi-open state, the simulation was started from the same structure as the production run of the Ca^{2+}-binding semi-open state, but with the Ca^{2+} cation deleted from EF3. For the closed state, we launched the simulation from the same structure as we did for the

direct production run. A total of 13 replicas of the system were simulated at 310 K with effective solute temperatures ranging from 310 K to 900 K (see Table SXA) and with exchanges of replicas being attempted every 2 ps. The average transition probabilities ranged from 0.21 to 0.36 for the neighboring pairs of effective solute temperatures. Importantly, the lowest effective solute temperature was frequently visited by replica geometries that had spent portions of their time in the high temperature range (see Fig. S9). Results were analyzed for the lowest effective solute temperature, sampling the statistical ensemble of interest. The first 100 ns of the production trajectories were not used for the analysis.

T_0	T_1	T_2	T_3	T_4	T_5	T_6	T_7	T_8	T_9	T_{10}	T_{11}	T_{12}
310	339	370	405	442	483	528	577	631	689	754	824	900

Table SXA. Solute temperatures [K] used in the REST2 simulations of recoverin.

Calculations of calcium affinities

Where not yet bound to recoverin, a Ca^{2+} ion was inserted into the simulation box by replacing a K^+ ion located near the EF3 loop. An additional K^+ ion was removed to compensate for the double positive charge of Ca^{2+}. A short (100 ps) targeted MD (TMD) simulation was conducted to bring the Ca^{2+} ion to an immediate proximity of EF3 (less than 0.8 nm from the center of mass of the EF3 loop). A 50 ns direct MD simulation was then performed to effectuate binding of the Ca^{2+} ion to the EF3 loop. Throughout this simulation, a wall potential imposed on the distance of the Ca^{2+} ion from the center of mass of the EF3 loop prevented the cation from moving farther than 0.8 nm from the EF3 loop. For certain structures (see the main text), the coordination number of the Ca^{2+} ion with the amino-acid residues of the EF3 loop was further enhanced by performing an additional 50 ns TMD simulation, followed by a 100 ns unrestrained equilibration run. In the former, a harmonic biasing potential was applied to the coordination number of the Ca^{2+} ion with the eight oxygen atoms of the EF3 loop known from the available NMR structures[11-12] to potentially coordinate Ca^{2+} in EF3. The force constant of the harmonic biasing potential, which was centered at a coordination number of 6,

was raised from 0 to 500 kJ/mol during the initial 2 ns of the TMD simulation, and it was maintained at this value for the remaining duration of the TMD run.

The standard free energies of Ca^{2+} binding were calculated on the basis of free-energy profiles obtained from replica-exchange umbrella sampling (REUS) simulations[13]. To preserve the overall conformation of the protein during the REUS simulation, the positions of all Cα atoms except those of the EF hand (i.e., residues 99–132 for binding to EF3 and 62–85 to EF2) were held fixed by employing harmonic position restraints with a force constant of 1000 kJ mol^{-1} nm^{-2}. The free-energy profiles were computed along a Cartesian component of the distance between the Ca^{2+} ion and the center of mass of the EF loop. Each REUS simulation comprised 20 umbrella windows spanning the range ~0–1.5 nm, with their initial geometries being extracted from a 2 ns pull run, performed with a force constant of 1000 kJ mol^{-1} nm^{-2}. The spacing (≤ 0.1 nm) between neighboring umbrella windows was adjusted so as to ensure a sufficiently high exchange rate (> 0.1). Exchanges of geometries between neighboring umbrella windows were attempted every 1 ps. The REUS simulations were propagated for a minimum of 40 ns and extended to up to 80 ns when required for the convergence of the free-energy profile. The strong binding of Ca^{2+} to the NMR structure of the semi-open state necessitated an additional REUS simulation with the collective variable restricted to the interval 0–0.5 nm and with the spacing between neighboring umbrella windows reduced to 0.01–0.05 nm. The umbrella histograms from this additional REUS simulation were combined with those from the original REUS simulation which were centered above 0.5 nm to obtain the free energy profile. All REUS simulations were performed in GROMACS 5.1.4[1] patched with the PLUMED 2.3.0 package.[10] The weighted histogram analysis (WHAM) method[14] was employed to construct the free energy profiles and the bootstrap analysis method[15] to estimate statistical errors.

To obtain standard binding free energies $\Delta G_{\mathrm{b}}^{\mathrm{o}}$ from the REUS free-energy profiles, we employed the following formula[16], in which an entropy term arising from a difference in the accessible volumes is subtracted from the potential of mean force,

$$\Delta G_{\mathrm{b}}^{\mathrm{o}} = \langle W(\boldsymbol{r}) \rangle_{\mathrm{b}} - k_{\mathrm{B}} T \ln\left(\frac{V_{\mathrm{b}}}{V^{\mathrm{o}}}\right) \quad \#(1)$$

In this expression, $\langle W(\boldsymbol{r})\rangle_{\mathrm{b}}$ is the ensemble average of the potential of mean force in the binding site, V_{b} denotes the volume of the binding site, and V^{o} = 1.66 nm^3 is the volume corresponding to the standard concentration C^{o} = 1 M. Unlike $W(\boldsymbol{r})$, the free-energy profiles $G(x)$ obtained from our REUS simulations (Figs. S15 and S16) already contain an entropic contribution corresponding to the accessible volume for the Ca^{2+} ion along the dissociation pathway,

$$G(x) = \langle W(\boldsymbol{r})\rangle_x - k_{\mathrm{B}}T\ \ln A(x)\ \#(2)$$

where $\langle W(\boldsymbol{r})\rangle_x$ is the ensemble average of $W(\boldsymbol{r})$ for a given value of the Cartesian coordinate x and $A(x)$ is the area of the volume slice, perpendicular to x, accessible to the Ca^{2+} ion. Thus, the average potential of mean force $\langle W(\boldsymbol{r})\rangle_{\mathrm{b}}$ in the binding site can be expressed as

$$\langle W(\boldsymbol{r})\rangle_{\mathrm{b}} = \Delta G + k_{\mathrm{B}}T\ \ln\frac{A_{\mathrm{b}}}{A_{\mathrm{f}}}\ \#(3)$$

Here ΔG is the difference between the value of $G(x)$ in the binding site and in bulk solution, and A_{b} and A_{f} are the accessible areas corresponding to the binding site and to bulk solution, respectively. Since the Ca^{2+} ion can move freely in bulk solution, A_{f} is equal to L^2, where L is the size of the simulation box. After inserting eq. 3 to eq. 1 and after additional manipulations, we arrive at our final expression for $\Delta G^{\mathrm{o}}_{\mathrm{b}}$,

$$\Delta G^{\mathrm{o}}_{\mathrm{b}} = \Delta G - k_{\mathrm{B}}T\left[\ln\left(\frac{l_{\mathrm{b}}}{L}\right) + \ln\left(\frac{L^3}{V^{\mathrm{o}}}\right)\right]\ \ \#(4)$$

where l_{b} is the length of the binding site along x. With $l_{\mathrm{b}} = 0.08$ nm, estimated from the RMSF of bound Ca^{2+}, and with an average box size of L = 8.5 nm in our simulations, eq. 4 yields a ΔG correction which is equal to –0.8 kcal/mol.

Calculations of spin relaxation rates

Spin relaxation rates for N-H backbone vectors were calculated from the Redfield equations,[17-18]

$$R_1 = \frac{d^2_{\mathrm{NH}}N_{\mathrm{H}}}{20}[J(\omega_{\mathrm{H}}-\omega_{\mathrm{N}}) + 3J(\omega_{\mathrm{N}}) + 6J(\omega_{\mathrm{N}}+\omega_{\mathrm{H}})] + \frac{(\Delta\sigma\omega_{\mathrm{N}})^2}{15}J(\omega_{\mathrm{N}})\ \#(5)$$

$$R_2 = \frac{d^2_{\mathrm{NH}}N_{\mathrm{H}}}{40}[4J(0) + J(\omega_{\mathrm{H}}-\omega_{\mathrm{N}}) + 3J(\omega_{\mathrm{N}}) + 6J(\omega_{\mathrm{H}}) + 6J(\omega_{\mathrm{N}}+\omega_{\mathrm{H}})] + \\ + \frac{(\Delta\sigma\omega_{\mathrm{N}})^2}{90}[4J(0) + 3J(\omega_{\mathrm{N}})]\#(6)$$

where ω_{H} and ω_{N} are the Larmor angular frequencies of ^{15}N and ^{1}H, respectively, d_{NH} denotes the dipolar coupling constant, $N_{\mathrm{H}} = 1$ is the number of bound protons for N-H bonds, $\Delta\sigma = -160$ ppm stands for the chemical shift anisotropy of N-H bonds in proteins, and $J(\omega)$ is the spectral density. $J(\omega)$ can be calculated as

$$J(\omega) = 2\int_0^{\infty} C(t)\cos(\omega t)\,dt \quad \#(7)$$

where $C(t)$ is the second order rotational correlation function for the N-H bond vector,

$$C(t) = \frac{3\langle\cos^2\theta_{t'+t}\rangle_{t'} - 1}{2} \#(8)$$

In this expression, $\theta_{t'+t}$ stands for the angle of the N-H bond between times t' and $t'+t$, and the angular brackets denote an average over t'. Before spin relaxation rate calculation, the rotational diffusion coefficients around the principal axes of inertia of the protein were divided by a factor of 3.2 to compensate for the overestimated overall protein rotational diffusion with TIP3P water model.[19-20] The factor 3.2 was chosen to optimize the agreement of R_2/R_1 ratio between the simulation and experiments for the Ca^{2+} free closed state, see Fig. S4. After scaling the overall rotational diffusion, the new rotational correlation functions were determined by taking into account the anisotropic shape of the protein as described in detail in Ref.[20]. To calculate the spectral density, we performed the fast Fourier transform of the new rotational function $C_{\mathrm{N}}(t)$, sampled at n discrete times t_m with a spacing of $\Delta t = 2$ ps,

$$J(\omega_k) = 2\,\mathrm{Re}\left[\sum_{m=0}^{n-1} C_{\mathrm{N}}(t_m)\exp(-i\omega_k t_m)\right]\Delta t \#(9)$$

where $\omega_k = 2\pi k/(n\Delta t)$. The values of $J(\omega)$ for $\omega \neq \omega_k$ were obtained by linear interpolation.

Supporting results

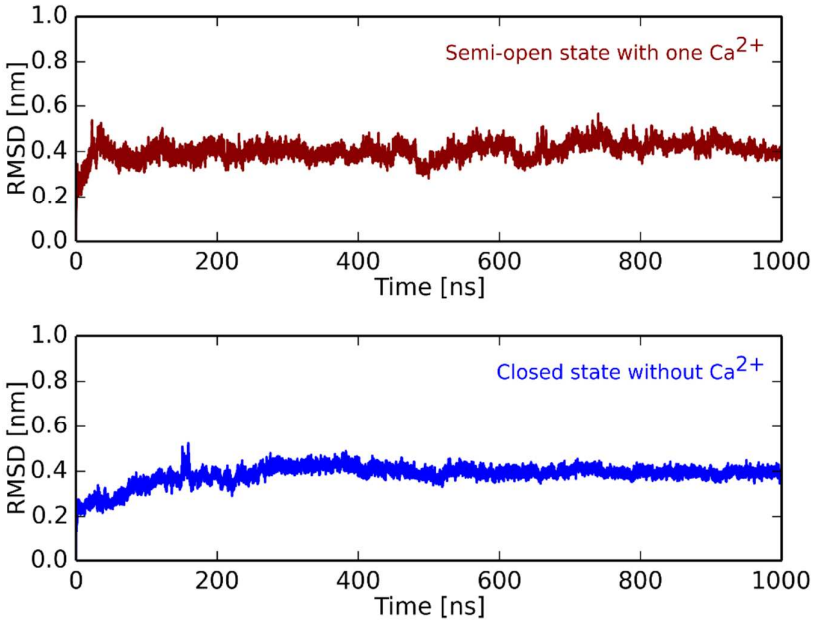

Figure S1. Cα RMSD from the initial structure during a 1 μs trajectory of the semi-open state loaded with one Ca^{2+} ion and during a 1 μs trajectory of the closed state without Ca^{2+}.

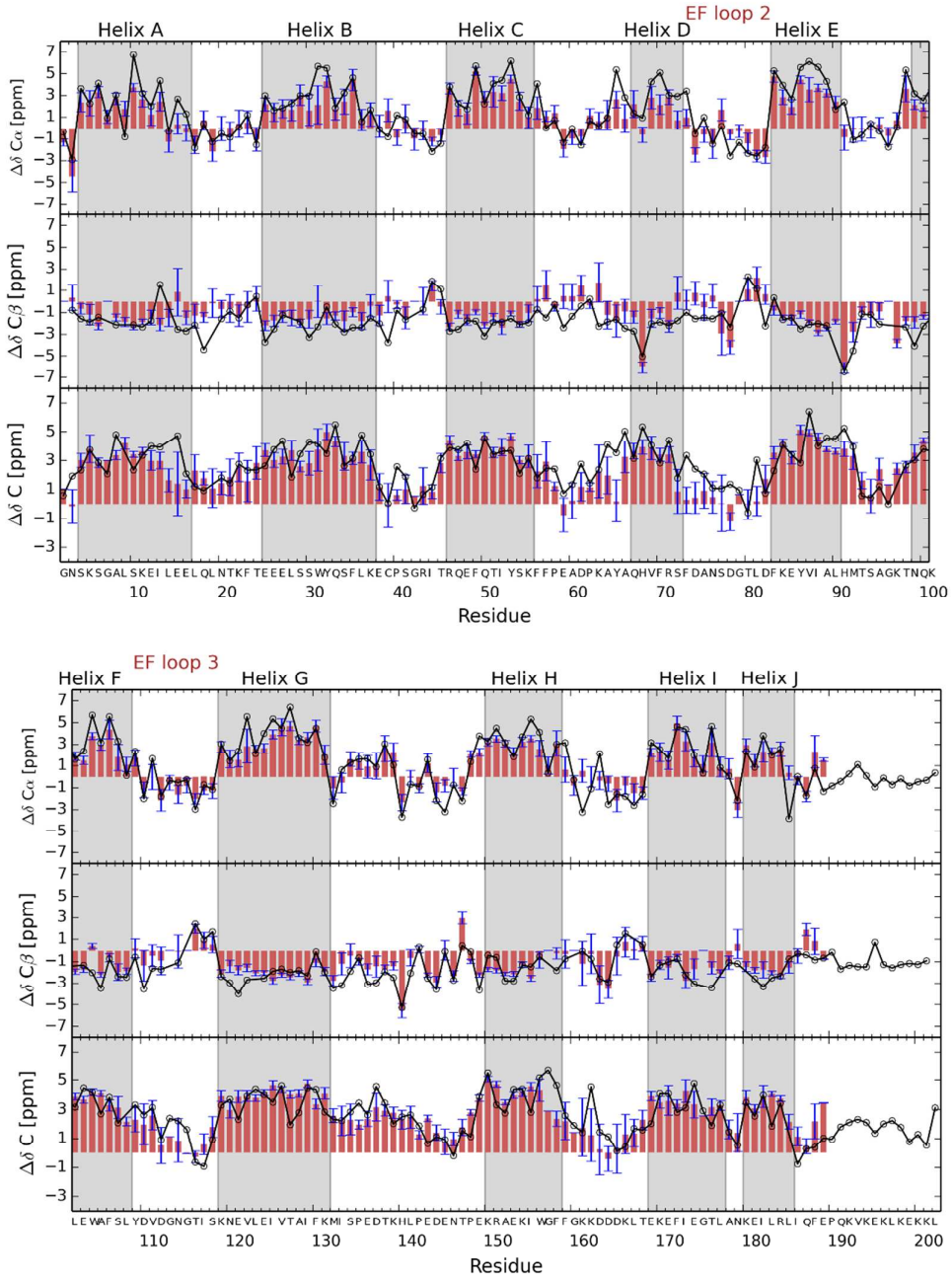

Figure S2. Secondary chemical shifts of the Ca^{2+}-free closed state of recoverin: A comparison between the simulation (red bars) and the experiment (black circles). The predicted values of Cα, Cβ, and C atom ^{13}C chemical shifts were calculated using the SHIFTX program[21] from 1000 snapshots extracted from a 1 μs trajectory. The experimental data come from Ref[22]. All chemical shifts are expressed relative to random coil chemical shifts calculated using an online script[23] for the amino acid sequence of recoverin at a temperature of 37 °C and at pH = 7.

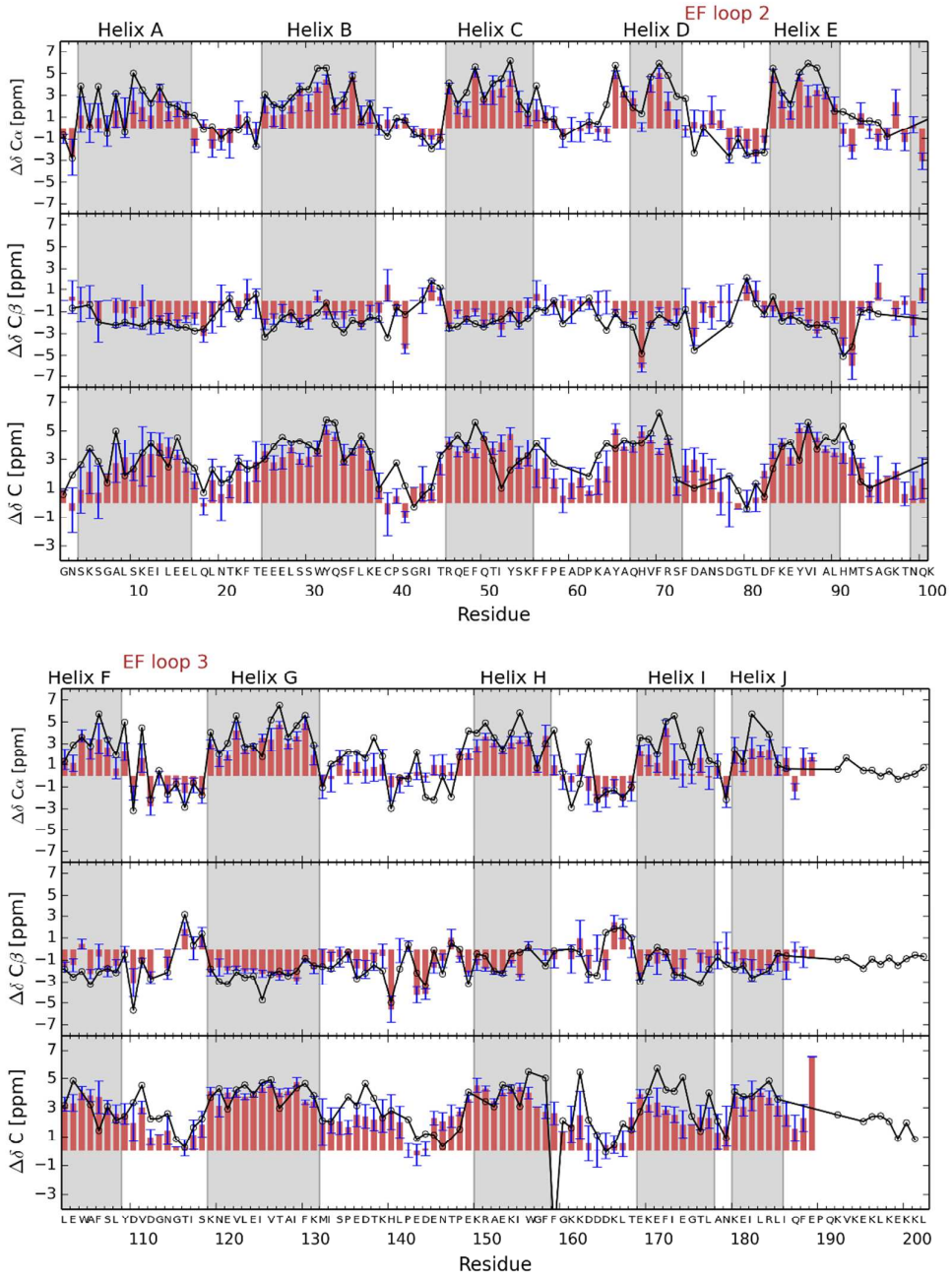

Figure S3. Secondary chemical shifts of the semi-open state of recoverin binding a single Ca^{2+} ion: A comparison between the simulation (red bars) and the experiment (black circles). The predicted values of Cα, Cβ, and C atom ^{13}C chemical shifts were calculated using the SHIFTX program[21] from 1000 snapshots extracted from a 1 μs trajectory. The experimental data come from Ref[11]. All chemical shifts are expressed relative to random coil chemical shifts calculated using an online script[23] for the amino acid sequence of recoverin at a temperature of 37 °C and at pH = 7.

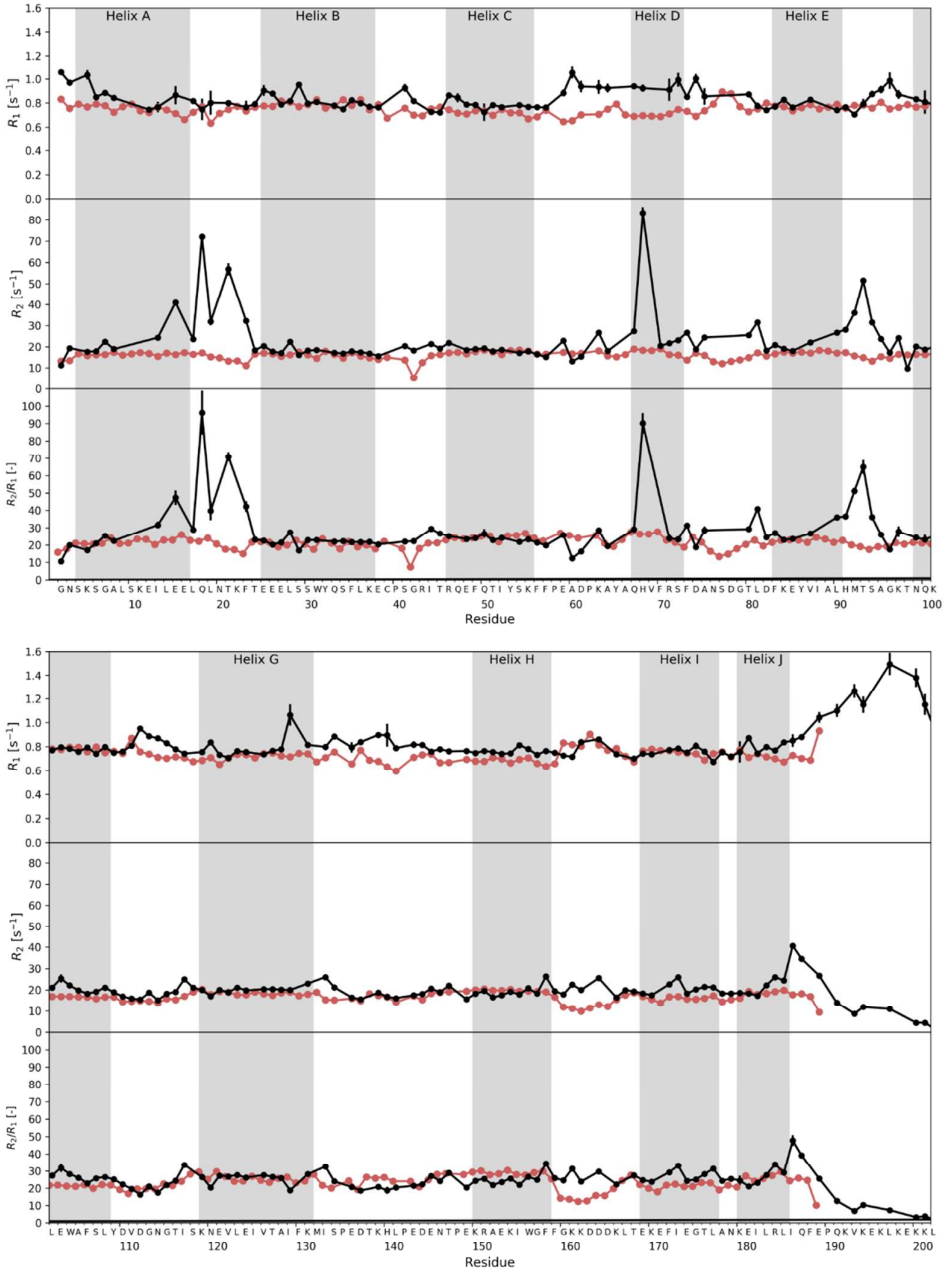

Figure S4. Longitudinal (R_1) and transverse (R_2) ^{15}N spin relaxation rates predicted from a 1 μs direct MD trajectory of the Ca^{2+}-free closed state (red circles) and compared with experimental values[24] (black circles) measured in the absence of Ca^{2+} at 81.08 MHz ^{15}N resonance frequency. The overall rotational diffusion coefficients of the protein are scaled with the factor of 3.2 to compensate for the overestimated rotational tumbling due to the TIP3P water model. Good agreement between simulations and experiments is found, except for the large R_2 values for residues 15, 18, 21, 68, 93, and 186, which were shown to arise from protein dynamics at the millisecond time scale using relaxation dispersion experiments[24]. The rotational diffusion coefficients given by the MD analysis ($D_{xx} = 1.3,\ D_{xx} = 1.2, D_{zz} = 1.6$ rad^2·10^7/s) suggest that the protein is slightly ellipsoidal. The timescale for the overall rotation ($\tau_c = (6D_{av})^{-1} = 12$ ns) is close to the estimate from the average R_2/R_1 ratio (15 ns)[24].

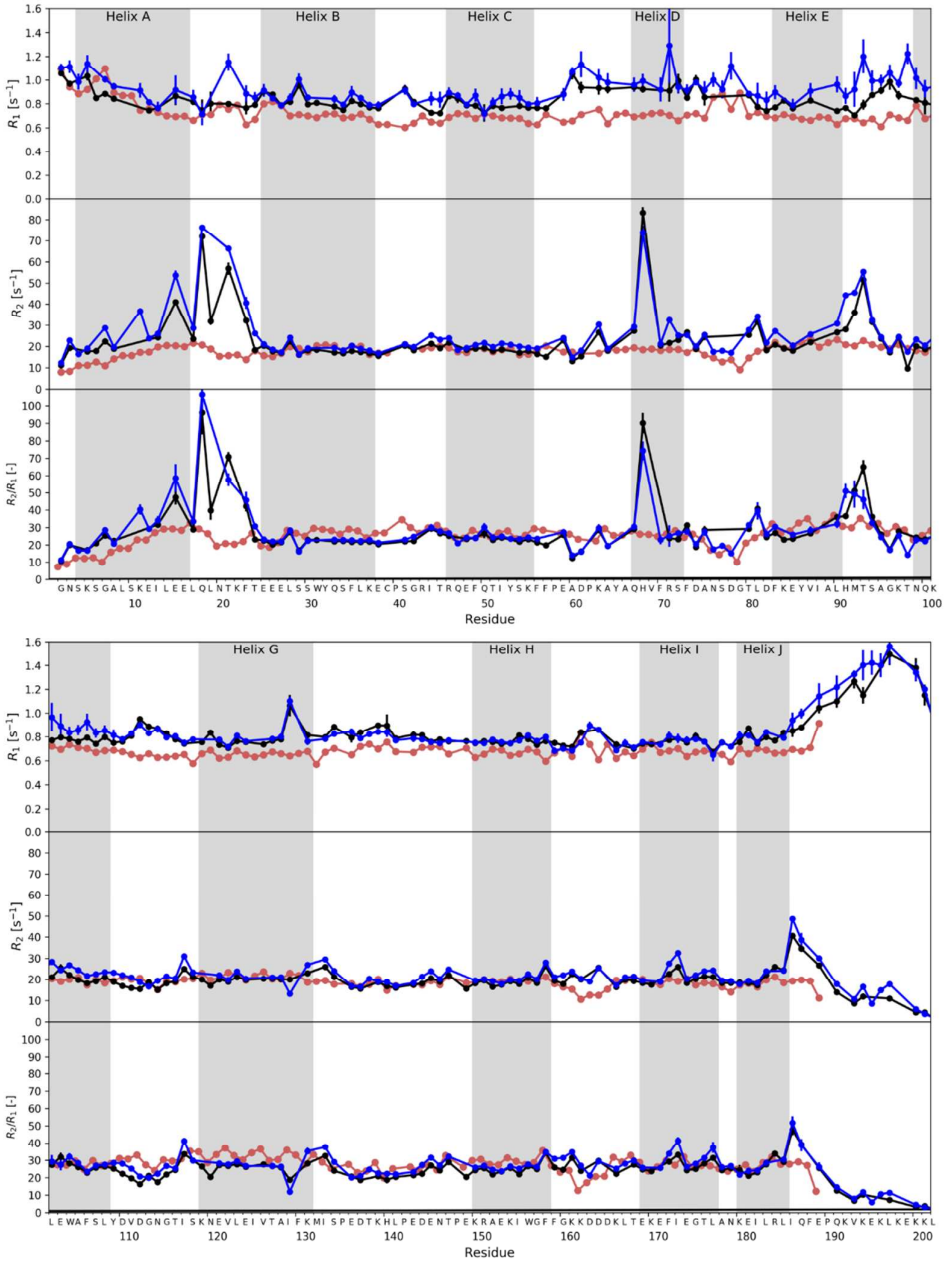

Figure S5. Longitudinal (R_1) and transverse (R_2) ^{15}N spin relaxation rates predicted from a 1 μs direct MD trajectory of the semi-open state binding a single Ca^{2+} ion (red circles). The values from MD are compared with experimental data[24] determined in the absence of Ca^{2+} (black circles) and at a 5% subsaturating Ca^{2+} concentration (blue circles) at 81.08 MHz ^{15}N resonance frequency. The overall rotational diffusion coefficients of the protein are scaled with the factor of 3.2 to compensate for the overestimated rotational tumbling due to the TIP3P water model. The rotational diffusion coefficients given by the MD analysis ($D_{xx} = D_{xx} = 1.1, D_{zz} = 1.6$ rad^2·10^7/s) suggest slightly more ellipsoidal shape and slightly slower rotational diffusion than for the Ca^{2+}-free closed state in Fig. S4. The timescale for the overall rotation ($\tau_c = (6D_{av})^{-1} = 13$ ns) is slightly longer than for the Ca^{2+}-free closed state, in agreement with the estimates from the average R_2/R_1 ratio (16 ns)[24].

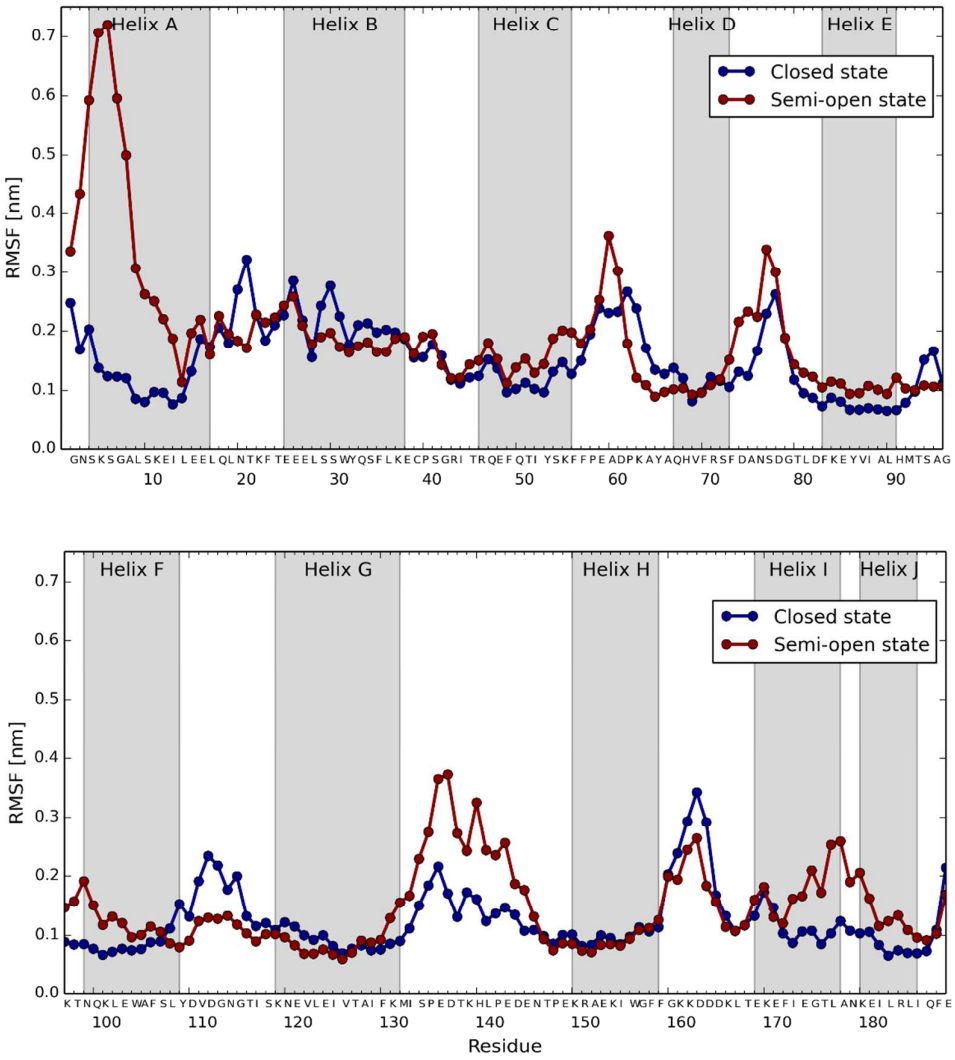

Figure S6. The N-terminus becomes destabilized owing to the domain rotation. A comparison of the root-mean-square fluctuations (RMSF) of Cα atoms in a 1 μs trajectory of the semi-open state binding one Ca^{2+} ion and in a 1 μs trajectory of the closed Ca^{2+}-free state of recoverin.

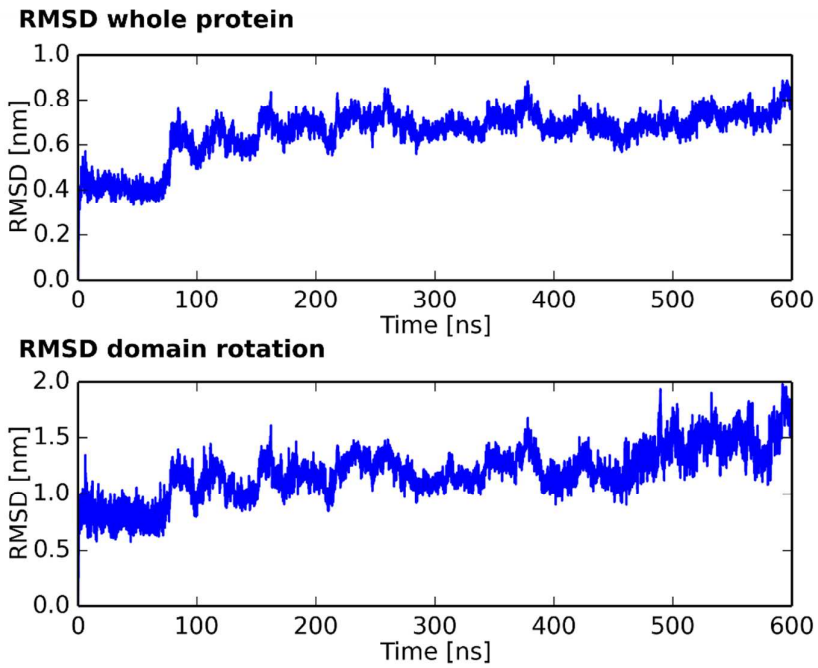

Figure S7. Ca^{2+} RMSD of the semi-open state after removing the Ca^{2+} ion bound in EF3. *(Top)* Ca^{2+} RMSD calculated for the whole protein after its alignment to the starting structure, *(bottom)* Ca^{2+} RMSD evaluated for the N-terminal domain (residues 2–91) after an alignment of the C-terminal domain (more specifically, residues 122–189) to the initial structure.

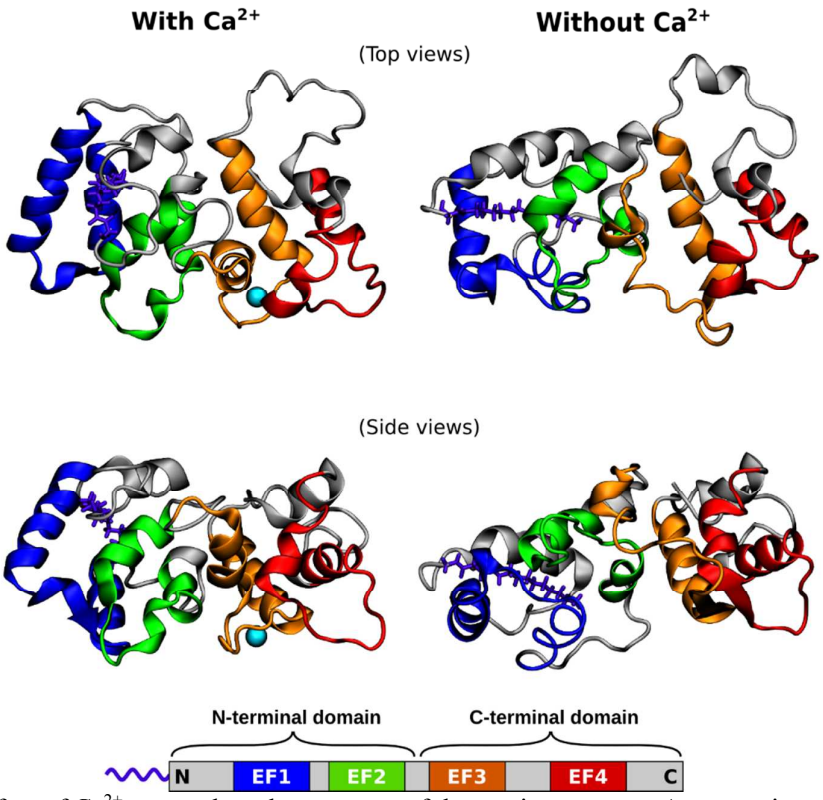

Figure S8. Effect of Ca^{2+} removal on the structure of the semi-open state. A comparison of a recoverin structure at the end of a 1 μs trajectory with a Ca^{2+} ion bound in EF3 *(left)* and at the end of a 600 ns trajectory without Ca^{2+} *(right)*. The C-domain residues 122–189 are superimposed for both structures.

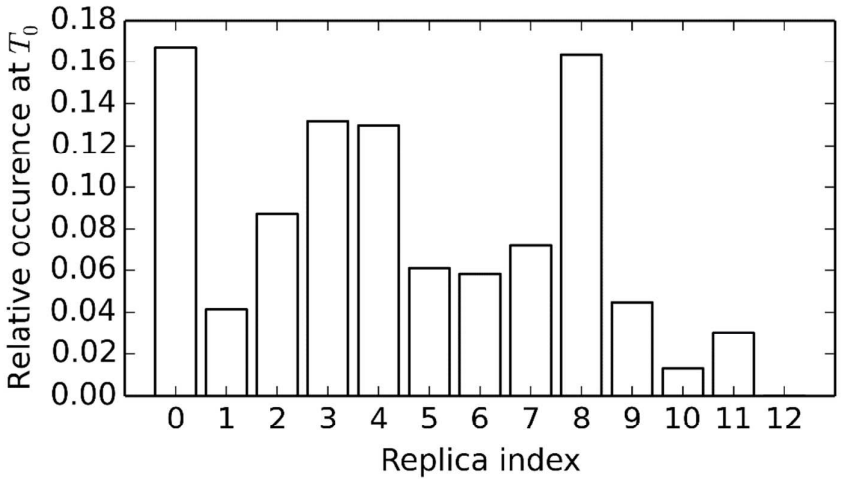

Figure S9. Occurrence of replicas at the lowest temperature T_0 in the REST2 simulation of the Ca^{2+}-free semi-open state.

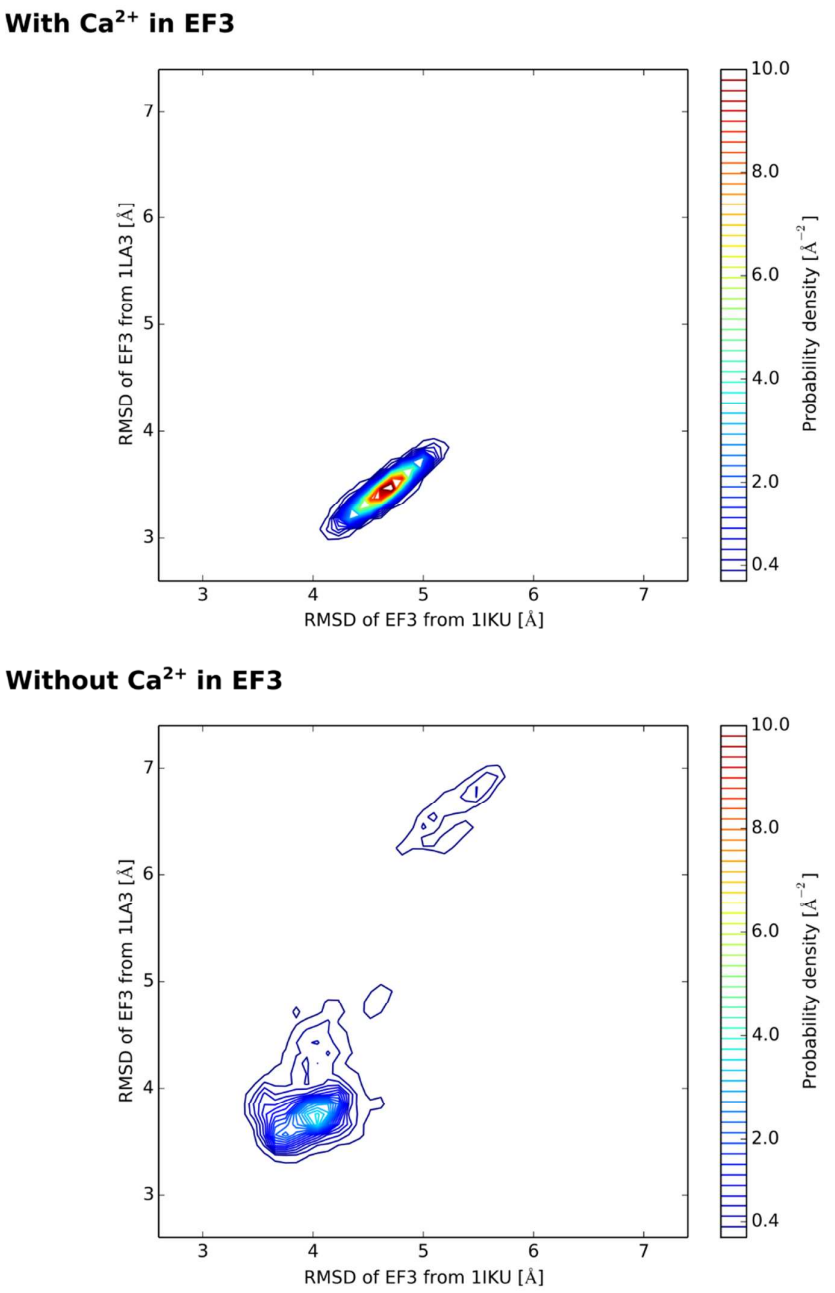

Figure S10. Removal of Ca^{2+} from EF3 changes the conformation of the EF hand. Comparison of Cα RMSD distances of the EF hand 3 from its conformations in the NMR structure of the closed state without Ca^{2+} (PDB ID 1IKU)[25] and in the NMR structure of the semi-open E85Q mutant (PDB ID 1LA3),[11] binding a Ca^{2+} ion in EF3. Results from a 1 μs direct MD trajectory of the semi-open state with Ca^{2+} *(top)* and from a 560 ns REST2 simulation of the semi-open state without Ca^{2+} *(bottom)*.

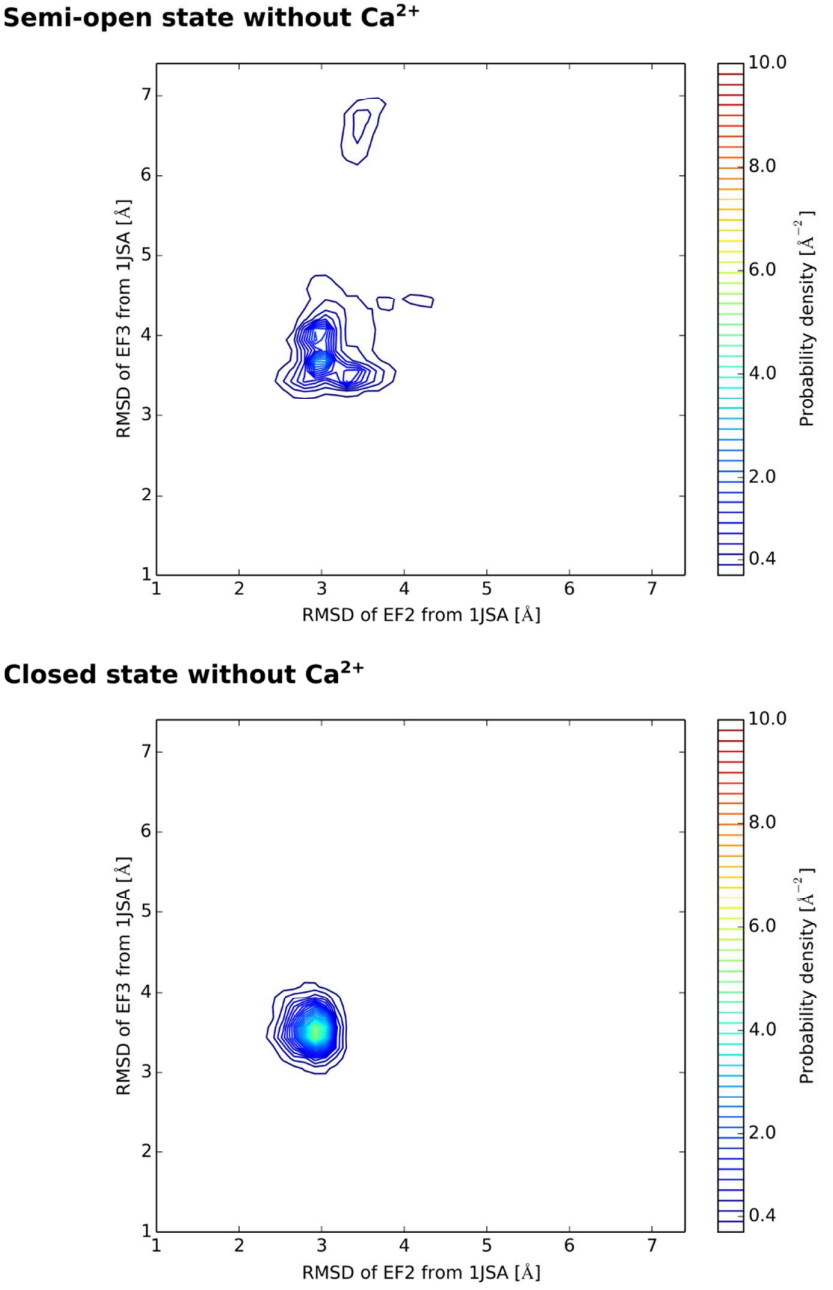

Figure S11. The EF hands 2 and 3 exhibit increased conformational variability in the Ca^{2+}-free semi-open state. Distribution of the Cα RMSD distances of the EF hands 2 and 3 from their conformations in the NMR structure of the open state (PDB ID 1JSA),[12] loaded with two Ca^{2+} ions. Results obtained from REST2 simulations of the semi-open state without Ca^{2+} *(top)* and of the closed state without Ca^{2+} *(bottom)*.

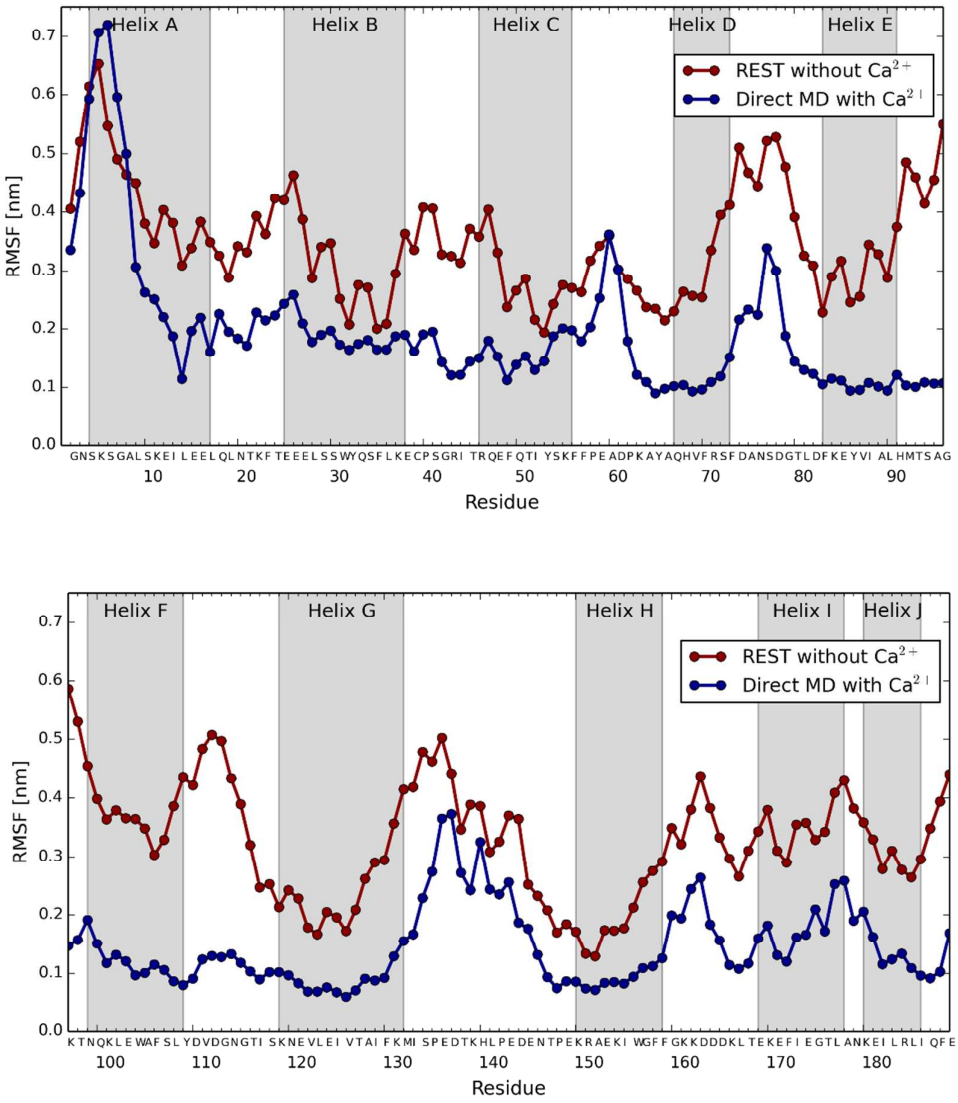

Figure S12. The REST2 simulation shows increased structural variation in the semi-open state of recoverin without Ca^{2+}. A comparison of the Cα RMSF values for the lowest temperature of a 560 ns REST2 simulation and for a 1 μs trajectory of the semi-open state binding one Ca^{2+} ion.

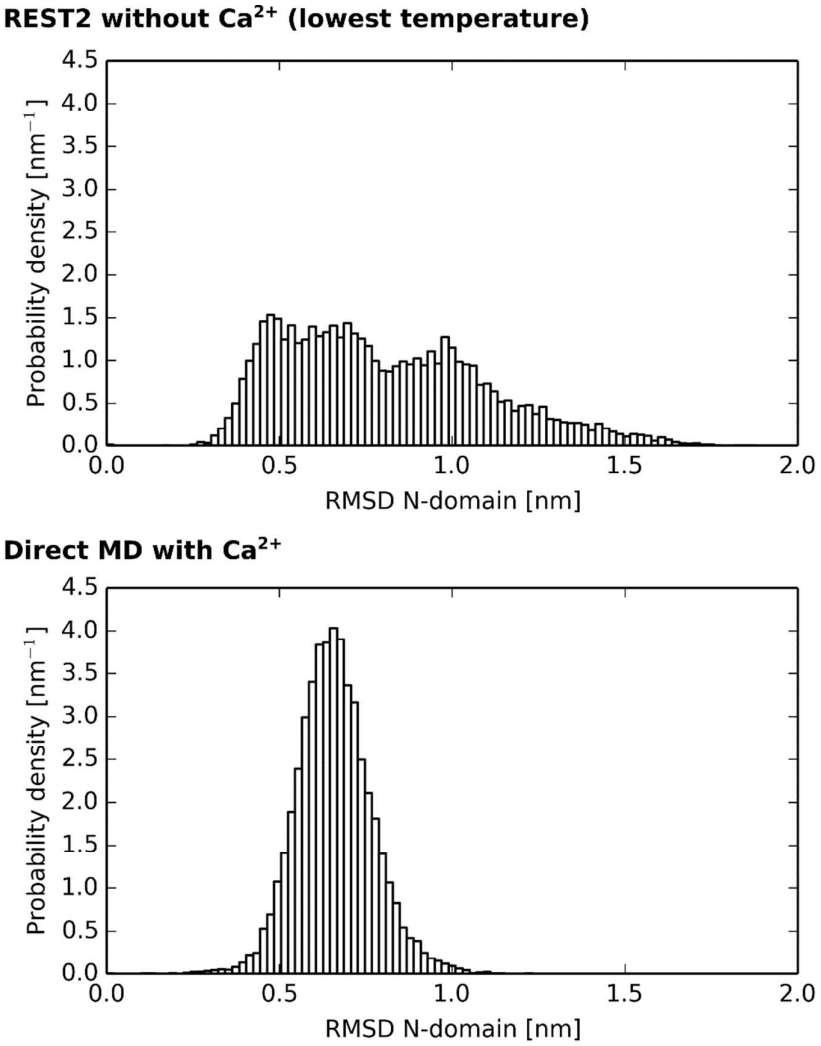

Figure S13. The absence of Ca^{2+} from EF3 translates into domain rotation. Histograms of Cα RMSD in the REST2 simulation without Ca^{2+} *(top)* and in direct MD with Ca^{2+} *(bottom)*, calculated for the N-terminal domain (residues 2–91) after an alignment of the C-terminal domain (residues 122–189) to the initial structure.

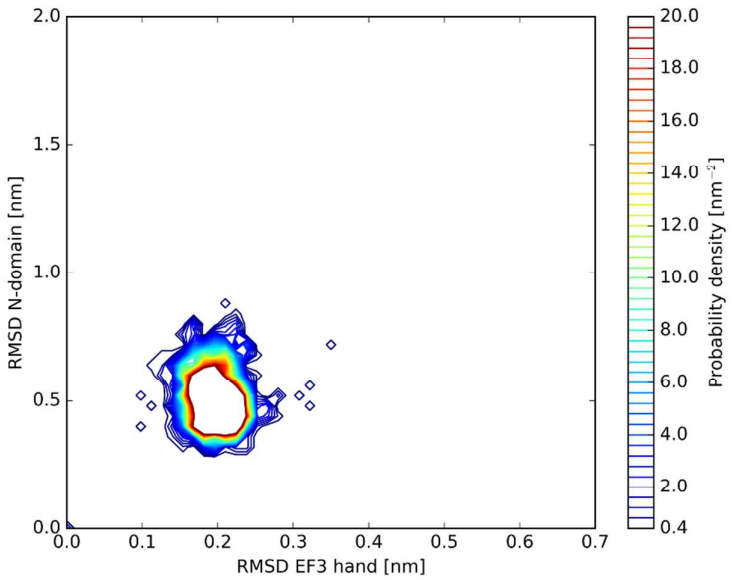

Figure S14. The closed state of recoverin is less variable in terms of its conformation than the semi-open state without Ca^{2+}. 2D histograms showing the correlation between the Cα RMSD of the EF hand 3 (residues 99–132) from its initial structure and the Cα RMSD of the N-terminal domain (residues 2–91) after an alignment of the C-terminal domain (residues 122–189) to the initial structure. The results were obtained from a REST2 simulation of the closed state without Ca^{2+}.

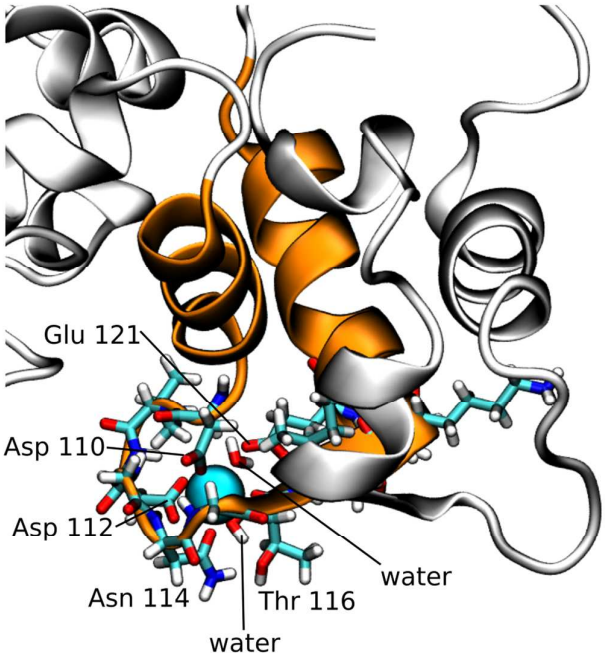

Figure S15. Ca^{2+} binding to the EF3 loop of the semi-open structure A. The side-chains of all the residues of the EF3 loop are shown. One of the two water molecules being in contact with Ca^{2+} forms a bridge between Ca^{2+} and the side-chain of Glu 121.

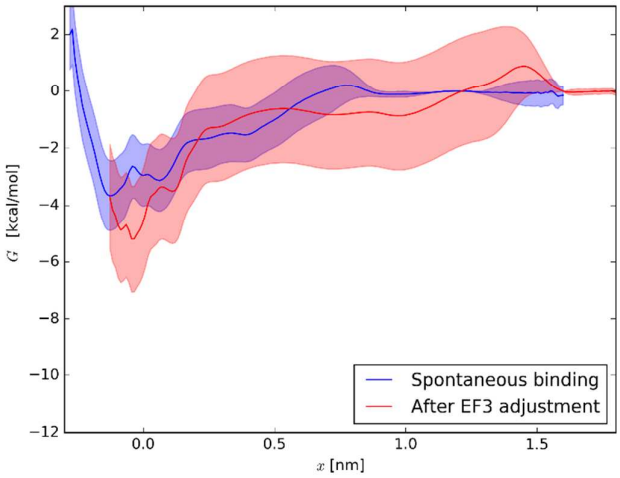

Figure S16. Free-energy profiles of calcium binding to EF3 in the closed state. Results from REUS simulations.

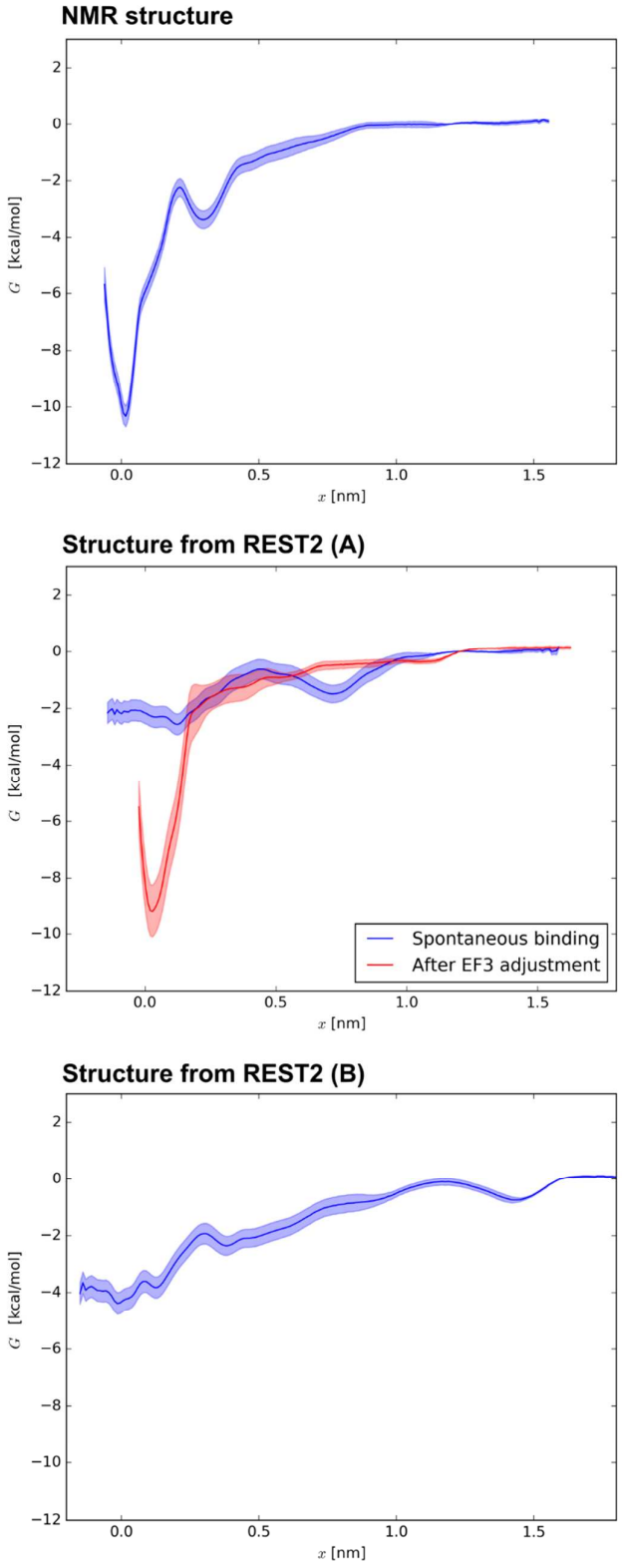

Figure S17. Free-energy profiles of calcium binding to EF3 in the semi-open state. Results from REUS simulations.

Supporting References

1. Abraham, M. J.; Murtola, T.; Schulz, R.; Páll, S.; Smith, J. C.; Hess, B.; Lindahl, E. Gromacs: High Performance Molecular Simulations through Multi-Level Parallelism from Laptops to Supercomputers. *SoftwareX* **2015,** *1–2*, 19-25.
2. Hockney, R. W.; Goel, S. P.; Eastwood, J. W. Quiet High-Resolution Computer Models of a Plasma. *J. Comp. Phys.* **1974,** *14*, 148-58.
3. Darden, T.; York, D.; Pedersen, L. Particle Mesh Ewald - an N.Log(N) Method for Ewald Sums in Large Systems. *J. Chem. Phys.* **1993,** *98*, 10089-92.
4. Hess, B.; Bekker, H.; Berendsen, H. J. C.; Fraaije, J. LINCS: A Linear Constraint Solver for Molecular Simulations. *J. Comput. Chem.* **1997,** *18*, 1463-72.
5. Miyamoto, S.; Kollman, P. A. Settle - an Analytical Version of the SHAKE and RATTLE Algorithm for Rigid Water Models. *J. Comput. Chem.* **1992,** *13*, 952-62.
6. Bussi, G.; Donadio, D.; Parrinello, M. Canonical Sampling through Velocity Rescaling. *J. Chem. Phys.* **2007,** *126*, 014101.
7. Parrinello, M.; Rahman, A. Polymorphic Transitions in Single-Crystals - a New Molecular-Dynamics Method. *J. Appl. Phys.* **1981,** *52*, 7182-90.
8. Berendsen, H. J. C.; Postma, J. P. M.; Vangunsteren, W. F.; Dinola, A.; Haak, J. R. Molecular Dynamics with Coupling to an External Bath. *J. Chem. Phys.* **1984,** *81*, 3684-3690.
9. Wang, L. L.; Friesner, R. A.; Berne, B. J. Replica Exchange with Solute Scaling: A More Efficient Version of Replica Exchange with Solute Tempering (REST2). *J. Phys. Chem. B* **2011,** *115*, 9431-9438.
10. Tribello, G. A.; Bonomi, M.; Branduardi, D.; Camilloni, C.; Bussi, G. PLUMED 2: New Feathers for an Old Bird. *Comput. Phys. Commun.* **2014,** *185*, 604-613.
11. Ames, J. B.; Hamasaki, N.; Molchanova, T. Structure and Calcium-Binding Studies of a Recoverin Mutant (E85Q) in an Allosteric Intermediate State. *Biochemistry* **2002,** *41*, 5776-5787.
12. Ames, J. B.; Ishima, R.; Tanaka, T. Molecular Mechanics of Calcium–Myristoyl Switches. *Nature* **1997,** *389*, 198-202.
13. Sugita, Y.; Akio, K.; Yuko, O. Multidimensional Replica-Exchange Method for Free-Energy Calculations. *J. Chem. Phys.* **2000,** *113*, 6042-6051.
14. Kumar, S.; Bouzida, D.; Swendsen, R. H.; Kollman, P. A.; Rosenberg, J. M. The Weighted Histogram Analysis Method for Free-Energy Calculations on Biomolecules. 1. The Method. *J. Comput. Chem.* **1992,** *13*, 1011-1021.
15. Hub, J. S.; de Groot, B. L.; van der Spoel, D. g_wham-a Free Weighted Histogram Analysis Implementation Including Robust Error and Autocorrelation Estimates. *J. Chem. Theory Comput.* **2010,** *6*, 3713-3720.
16. Zhou, H.-X.; Gilson, M. K. Theory of Free Energy and Entropy in Noncovalent Binding. *Chem. Rev.* **2009,** *109*, 4092-4107.
17. Abragam, A. *The Principles of Nuclear Magnetism*. Oxford University Press: 1961.
18. Kay, L. E.; Torchia, D. A.; Bax, A. Backbone Dynamics of Proteins as Studied by Nitrogen-15 Inverse Detected Heteronuclear NMRSpectroscopy: Application to Staphylococcal Nuclease. *Biochemistry* **1989,** *28*, 8972-8979.
19. Wong, V.; Case, D. A. Evaluating Rotational Diffusion from Protein MD Simulations. *J. Phys. Chem. B* **2008,** *112*, 6013-6024.
20. Ollila, O. H. S.; Heikkinen, H.; Iwai, H. Rotational Dynamics of Proteins from Spin Relaxation Times and Molecular Dynamics Simulations. *In preparation*.
21. Neal, S.; Nip, A. M.; Zhang, H. Y.; Wishart, D. S. Rapid and Accurate Calculation of Protein H-1, C-13 and N-15 Chemical Shifts. *J. Biomol. NMR* **2003,** *26*, 215-240.
22. Tanaka, T.; Ames, J. B.; Kainosho, M.; Stryer, L.; Ikura, M. Differential Isotype Labeling Strategy for Determining the Structure of Myristoylated Recoverin by NMR Spectroscopy. *J. Biomol. NMR* **1998,** *11*, 135-152.
23. Maltsev, A. Random Coil Chemical Shifts for Intrinsically Disordered Proteins. http://www1.bio.ku.dk/english/research/bms/research/sbinlab/groups/mak/randomcoil/script/.

24. Xu, X.; Ishima, R.; Ames, J. B. Conformational Dynamics of Recoverin's Ca^{2+}-Myristoyl Switch Probed by ^{15}N NMR Relaxation Dispersion and Chemical Shift Analysis. *Proteins* **2011,** *79*, 1910-1922.
25. Tanaka, T.; Ames, J. B.; Harvey, T. S.; Stryer, L.; Ikura, M. Sequestration of the Membrane-Targeting Myristoyl Group of Recoverin in the Calcium-Free State. *Nature* **1995,** *376*, 444-447.